

STRUCTURE AND LUMINESCENCE PROPERTIES OF POROUS ALUMINA TEMPLATES DOPED WITH RARE EARTH ELEMENTS AND TRANSITION METALS

M. Enachi¹, V. Trofim¹, V. Coseac², I.M. Tiginyanu^{1,3}, and V.V. Ursaki³

¹*Technical University of Moldova, 168, Stefan cel Mare ave., MD-2004,
Chisinau, Republic of Moldova*

²*Academy of Transport, Informatics, and Communications, 121a, Muncesti str., MD-2002,
Chisinau, Moldova*

³*Institute of Applied Physics, Academy of Sciences of Moldova, 5, Academiei str., MD-2028,
Chisinau, Republic of Moldova*

(Received 25 September 2008)

Abstract

We propose to develop phosphor materials on the basis of porous alumina templates doped with rare earth elements and transition metals. This issue is especially important in connection with the development of random lasers, since the scattering properties of the porous template can be controlled by tailoring its morphology. In this work, we demonstrate that, apart from the morphology, the crystallographic structure of the template can be controlled by the conditions of post-anodization thermal treatment applied for the activation of the impurity impregnated from rare earth or transition metal containing solutions. The initially amorphous alumina structure is transformed into a γ -Al₂O₃ phase by annealing at 300–700°C. A δ -Al₂O₃ phase is predominant in samples annealed at 800–1000°C. The samples annealed at temperatures above 1100°C exhibit an α -Al₂O₃ structure. The technological conditions related to the solution concentration and duration of impregnation, postimpregnation annealing temperature and annealing duration were optimized from the point of view of maximum impurity ion activation.

1. Introduction

The development of power electronics depends on the progress in miniaturization of electronic components. However, the limitations of the state of the art fabrication techniques become an obstacle for the scaling down of conventional technologies. The interest in nanometer-scale materials and devices stimulated the development of alternative technologies in recent years. The implementation of dielectric and semiconductor templates in nanofabrication is one of the alternative approaches. Anodic porous alumina is the most widely used template [1-3]. The nanopores in the template are formed by anodizing aluminum films in an acidic electrolyte. We propose to use porous alumina templates as a host for doping rare earth elements and transition metals and the preparation of phosphor materials. Taking into account the possibility to control the morphology and porosity of the anodic porous alumina template and therefore to control its light scattering properties, this problem becomes especially important in connection with the growing interest in the development of random lasers (see, e.g., [4] and refs therein).

A random laser comprises two basic elements: an electromagnetic radiation emitting and amplifying phase and an electromagnetic radiation scattering phase [5]. In some cases the two functions are accomplished by the same phase. The stimulated emission may come from

the transition metals and rare earth elements doped into the radiation emitting and amplifying phase such as neodymium related electronic transitions in laser crystal powders doped with neodymium [6-8]. Recently, an attempt has been undertaken to dope Eu ions into a porous GaP or GaAs template [9, 10]. However, the annealing necessary for the activation of the impurity leads to the oxidation of the template, which may result in changing its morphology. This may complicate the control of the light scattering properties. Anodic porous alumina templates are more stable against annealing; therefore, one avoids complications with the uncontrolled change of the morphology.

The goal of this paper is to demonstrate the advantages of developed phosphor materials on the basis of porous alumina templates doped with rare earth elements and transition metals. We analyze the evolution of crystallographic structure of the template during the post-anodization thermal treatment applied for the activation of the doped impurity and identify the optimum technological conditions for the impurity ion activation.

2. Technological aspects and morphology characterization

The preparation of porous alumina templates consists in electrochemical oxidation of Al foils. This technology allows one to prepare two-dimensional Al_2O_3 templates with the size of pores ranging from 30 to 200 nm. Electrochemical etching in various electrolytes, such as aqueous solutions of H_3PO_4 , H_2SO_4 , and oxalic acid, was used. The morphology and the chemical composition microanalysis of etched samples were studied using a TESCAN scanning electron microscope (SEM) equipped with an Oxford Instruments INCA energy dispersive X-ray (EDX) system.

It was found that etching in 3 ml H_2SO_4 dissolved into 100 ml of water at the applied voltage of 30 V results in the formation of pores with the diameter of 25 nm. A template with the thickness of 100 nm is produced during 1-hour treatment (Fig. 1a). Electrochemical treatment in solutions consisting of 2 g of oxalic acid and 100 ml of water at a voltage of 100 V allows one to obtain pores of 50 nm (Fig. 1b). A template with the thickness of 40 μm is produced during 40-min treatment. In order to produce pores with bigger diameter, it is necessary to use H_3PO_4 electrolytes. Figure 1c illustrates a template produced by etching in a solution containing 8 ml H_3PO_4 , 100 ml water, and 5 g of NaOH at a voltage of 100 V. This treatment results in the formation of pores with a diameter of 150–200 nm.

Electrochemical treatment in H_2SO_4 and oxalic acid with the above mentioned conditions leads to a very low porosity of around 10%, while treatment in H_3PO_4 solutions, on the contrary, results in a high enough degree of porosity around 60%.

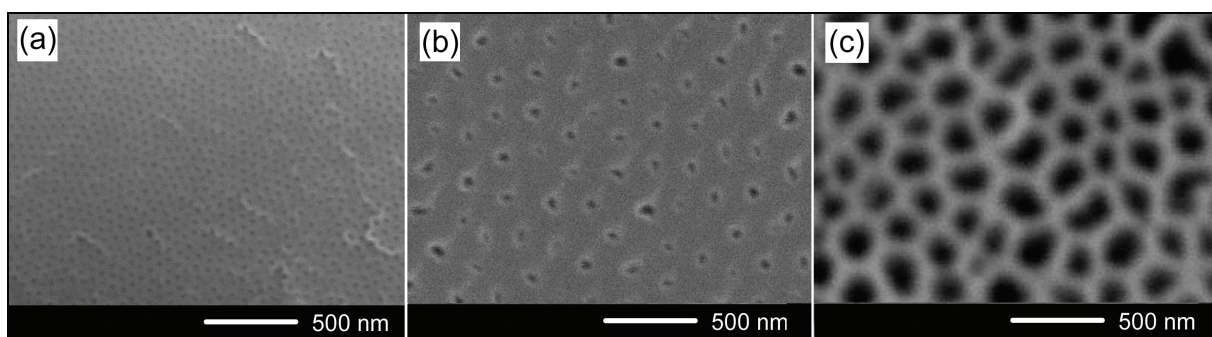


Fig. 1. Al_2O_3 templates produced by etching of Al foils in H_2SO_4 (a); oxalic acid (b); and H_3PO_4 (c) aqueous solutions.

Electrochemical treatment of Al foils is also suitable to produce alumina nanotubes. With treatment in H_3PO_4 aqueous solutions, one can obtain nanotubes with the diameter of 200 nm as shown in Fig. 2 (left). Nanotubes with small diameters of 50 nm are produced with treatment in a solution of $NiSO_4 \cdot 7H_2O$ (2g) in water (100 ml) at applied voltage of 40 V (Fig. 2, right).

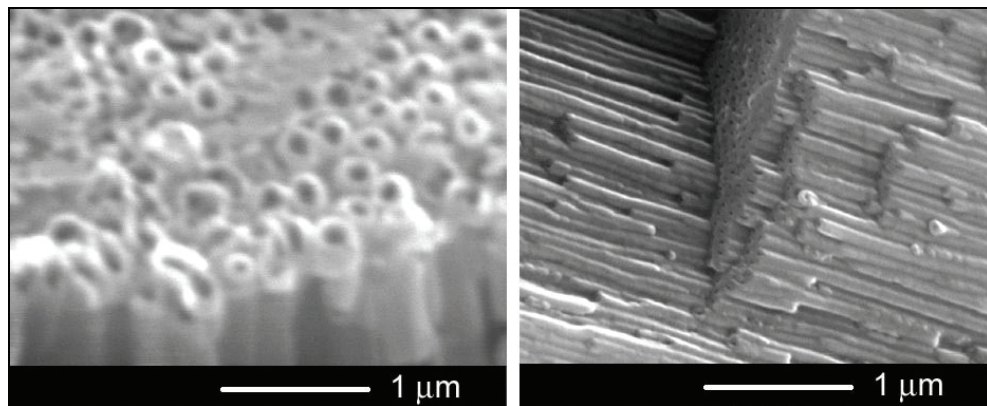


Fig. 2. Al_2O_3 nanotubes produced by etching of Al foils in H_3PO_4 (a) and $NiSO_4 \cdot 7H_2O$ aqueous solutions.

The technology for doping of porous alumina templates with rare earth and transition metal elements includes impregnation of Eu^{3+} and Cr^{3+} ions from $EuCl_3:C_2H_5OH$ and aqueous $CrCl_3 \cdot 6H_2O$ solutions, respectively. After impregnation, the samples are annealed for one hour at temperatures in the range from 500 to 1100°C in Ar.

3. Crystallographic structure characterization

Annealing applied for activation of the rare earth and transition metal impurities into Al_2O_3 templates leads to various transformations of the crystallographic structure (see Fig. 3).

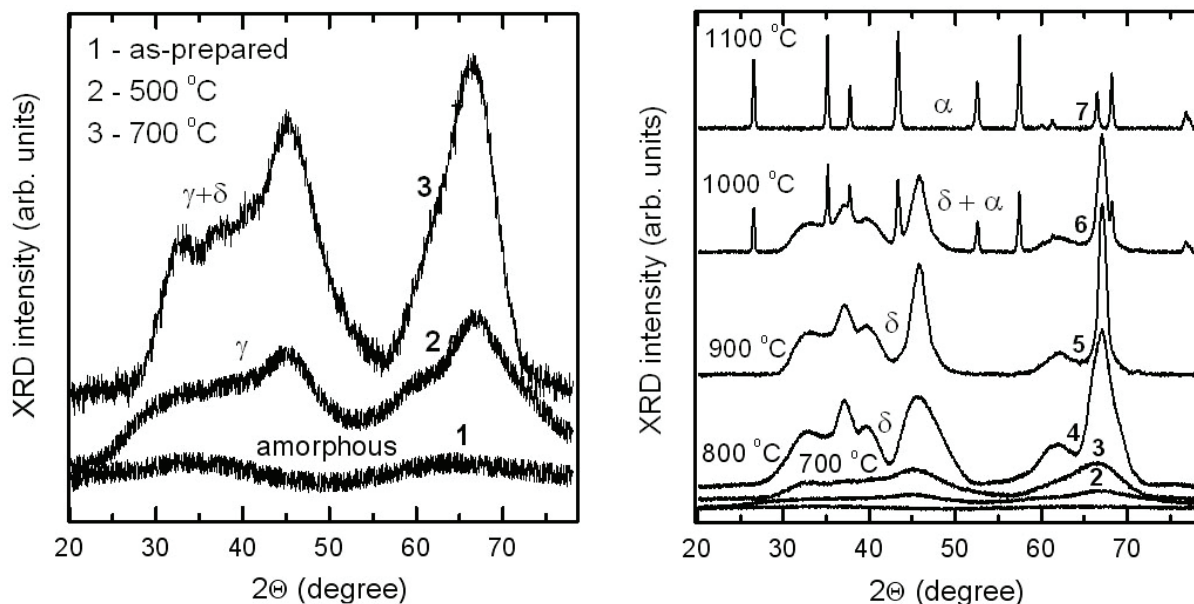


Fig. 3. Crystallographic structure of alumina templates annealed at different temperatures up to 700°C (left) with the extended y-axis and up to 1100°C (right).

The initially amorphous alumina structure is transformed into a $\gamma\text{-Al}_2\text{O}_3$ phase by annealing at 300–700°C. A $\delta\text{-Al}_2\text{O}_3$ phase is predominant in samples annealed at 800–1000°C. The samples annealed at temperatures above 1100°C exhibit an $\alpha\text{-Al}_2\text{O}_3$ structure.

4. Characterization of light scattering properties

The photonic strength of the scattering medium is defined in terms of the transport mean free path l_t , which is the average length required to randomize the direction of propagation of the light by scattering. A small value of l_t corresponds to efficient scattering or high photonic strength. To characterize the photonic strength of the samples, the transport mean-free path l_t is deduced from enhanced backscattering EBS measurements [11].

The EBS measurements were performed with a He:Ne laser as light source ($\lambda = 633$ nm). The measured angular dependence of the backscattering for Al_2O_3 samples with morphologies illustrated in Fig. 1 is shown in Fig. 4.

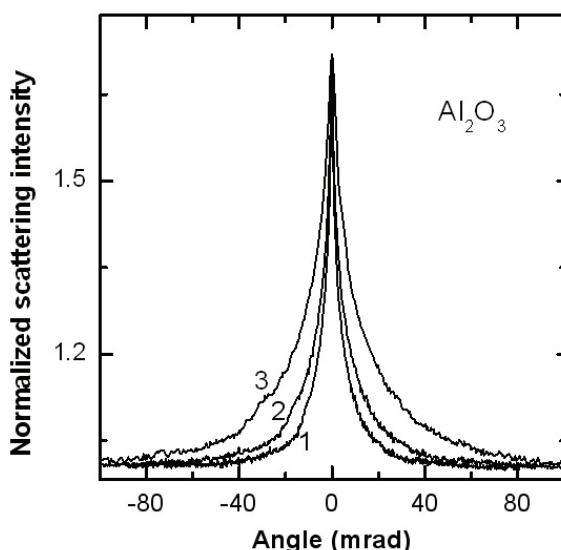


Fig. 4. The measured angular dependence of the backscattering for Al_2O_3 samples with the morphology illustrated in Figs. 1a (curve 1), 1b (curve 2), and 1c (curve 3).

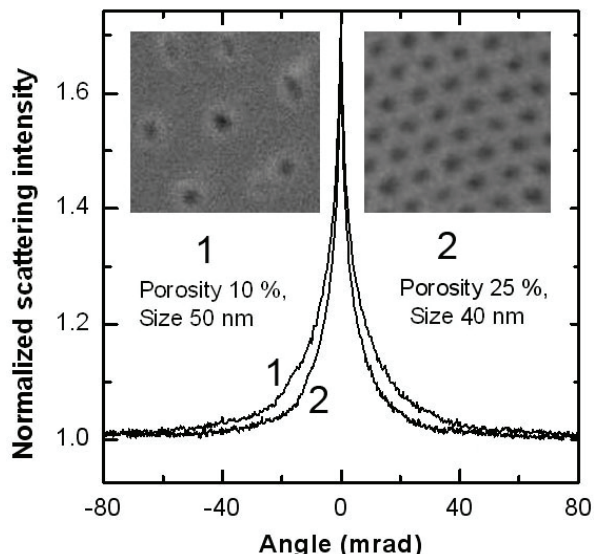


Fig. 5. The measured angular dependence of the backscattering for Al_2O_3 samples with the morphology illustrated in inset. The size of images 1 and 2 is 500 x 500 nm and 400 x 400 nm, respectively.

The full width at half maximum W of the EBS cone is directly related to the transport mean free path l_t . For a nonabsorbing and semi-infinite sample, this relation is $l_t = 0.7\lambda(1-R)/2\pi W$ [12], where R is the angular and polarization-averaged internal reflection at the sample boundary.

The measured value of W increases from 3 mrad to 6 mrad when comparing the samples with the morphology shown in Figs. 1a and 1b. The calculated transport mean-free path decreases from 9.4 μm to 4.7 μm . Since the porosity of these samples is nearly the same (around 10%), one can conclude that the decrease in the transport mean-free path is due to the increase in the characteristic size of the nanostructure from 25 nm to 50 nm.

The further increase in the characteristic size of the nanostructure from 50 nm (Fig. 1b) to 300 nm (Fig. 1c) leads to the increase in the value of W from 6 mrad to 13 mrad. However, the calculated value of the transport mean-free path decreases only from 4.7 μm to 3.8 μm . This is

due to the decrease in the effective refractive index induced by increased porosity. The decrease in the effective refractive index leads to the decrease in the reflectivity from 60% to 30%.

In order to verify the influence of the porosity on the transport mean-free path, we prepared samples with nearly the same diameter of pores, but with significantly different porosity. The treatment of Al foils in 5 ml H₂SO₄ dissolved into 100 ml of water at the applied voltage of 40 V was found to result in the formation of pores with the diameter around 40 nm (see image 2 in Fig. 5) which is close to the diameter of pores produced by treatment in solutions consisting of 2 g of oxalic acid and 100 ml of water at a voltage of 100 V (see image 1 in Fig. 5). However, the porosity of the sample with image 2 is around 25% against 10% porosity of the sample with image 1. The measured value of W decreases from 6 mrad to 4 mrad when comparing the samples with morphology 1 and 2, respectively. However, the increase of the transport mean-free path is more significant (from 4.7 μm to 8.8 μm) due to the decrease in the effective refractive index induced by the increase in the porosity, and the decrease in the reflectivity from 60% to 50%.

Annealing of porous alumina samples up to temperatures of 700°C was found to lead to the increase in the photonic strength (the decrease in the transport mean-free path), while the further increase in the annealing temperature leads to the decrease in the photonic strength. This behavior of the photonic strength with annealing is partially due to the phase transformations induced by annealing, partially due to the change in the morphology of samples (at high annealing temperatures).

5. Luminescence characterization

Photoluminescence (PL) was excited by different lines of an Ar⁺ SpectraPhysics laser and analyzed through a double spectrometer at room temperature. The resolution was better than 0.5 meV.

Figures 6 and 7 illustrate the PL spectra of alumina templates doped with different concentrations of Eu ions annealed at 800°C and of samples doped with Cr ions and annealed at different temperatures. The emission lines corresponding to the Eu³⁺ and Cr³⁺ intrashell transitions are well resolved in the PL spectra.

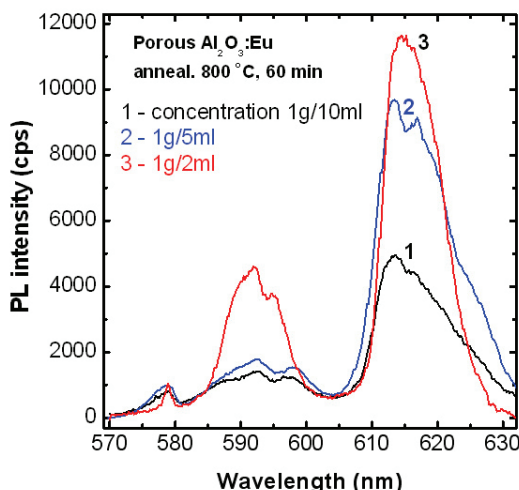


Fig. 6. PL spectra of porous alumina templates doped with various concentrations of Eu.

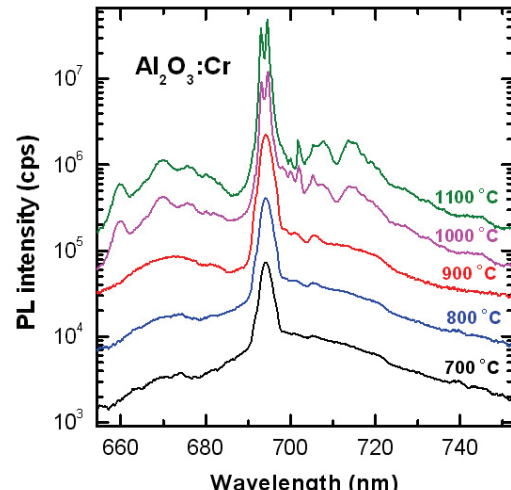


Fig. 7. PL spectra of porous alumina templates doped with Cr from a solution with the concentration of 1g/5ml annealed at different temperatures.

Analysis of the luminescence intensity under excitation by different laser lines has shown that the highest luminescence intensity from samples doped with Eu is observed under excitation by the 465.8 nm laser line. The fact that the quantum energy of these lines corresponds exactly to $^5D_2 \leftarrow ^7F_0$ transitions in Eu^{3+} ions, suggests that the excitation occurs via this transition, followed by non-radiative relaxation to the lower 5D_0 energy states. From these states, radiative transitions to the ground $^7F_{1-4}$ states occur.

Two narrow lines at 693.1 and 694.6 nm observed in the spectra of alumina templates doped with Cr and annealed at high temperatures are the so-called R-lines [13], which result from the $^2E \rightarrow ^4A_2$ $3d$ intrashell transition of Cr^{3+} ions and the splitting of the 2E level due to crystal field and spin-orbit interaction. These two lines correspond to $^2E(E) \rightarrow ^4A_2$ and $^2E(2\bar{A}) \rightarrow ^4A_2$ transitions.

The dependence of the luminescence intensity on the technological conditions of preparation of alumina templates doped with Eu and Cr is shown in Figs. 8 and 9.

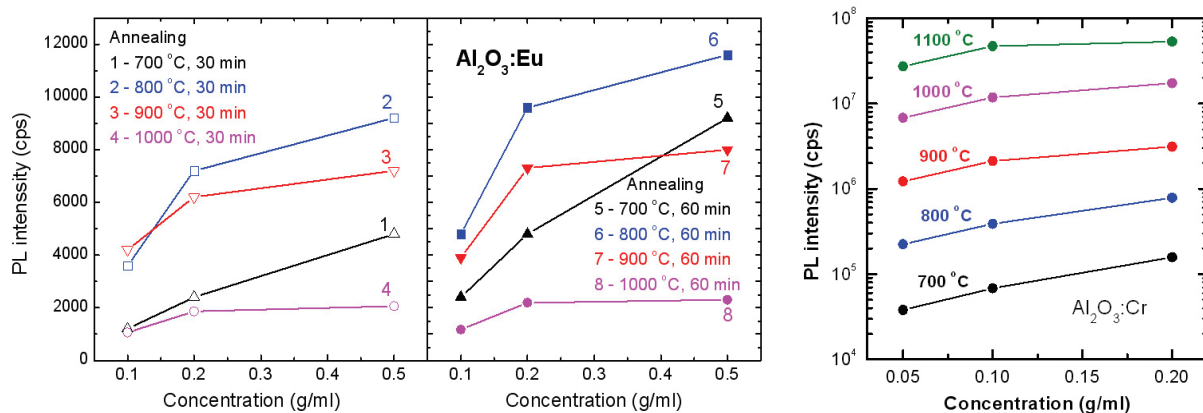


Fig. 8. Dependence of the PL intensity of alumina templates doped with Eu upon the technological conditions.

Fig. 9. Dependence of the PL intensity of alumina templates doped with Cr upon the technological conditions.

The analysis in Fig. 8 demonstrates that the intensity of luminescence in samples doped with Eu increases with the temperature increasing up to 800°C. Further increase in annealing temperature leads to the decrease in the luminescence intensity. This decrease is especially sharp at annealing temperatures higher than 1000°C, i.e., at temperatures corresponding to the formation of α - Al_2O_3 phase. This means that Eu ions are well activated in the γ and δ alumina phases, while they are hardly activated in the α -phase. In contrast to this, the luminescence intensity related to Cr ions monotonously increases with annealing temperature up to 1100°C. This is indicative of an efficient activation of Cr ions into the α -alumina host.

6. Conclusions

The results of this work demonstrate the possibility to develop phosphor materials with controlled light emission and light scattering properties on the basis of porous alumina templates doped with rare earth elements and transition metals. The thermal treatment applied for the activation of the impurity impregnated in porous alumina templates from rare earth or transition metal containing solutions leads to various crystallographic transformations. Eu ions are more efficiently activated in γ and δ alumina phases which are formed at annealing temperatures in an interval of 700-900°C, while Cr ions prove to be efficiently activated in the α - Al_2O_3 phase formed at annealing temperatures above 1000°C.

Acknowledgments

This work was supported by STCU under Grant # 4034.

References

- [1] C.R. Martin, *Science*, 266, 1961, (1994).
- [2] D. Routkevitch, A.A. Tager, J. Haruyama, D. Almawlawi, M. Moskovits, and J.M. Xu, *IEEE Transactions on Electron Devices*, 43, 1646, (1996).
- [3] H. He and N.J. Tao, *Encyclopedia of Nanoscience and Nanotechnology*, ed. by H.S. Nalwa, American Scientific Publishers, 10, 1–18, 2003.
- [4] H. Cao, in *Progress in Optics*, E. Wolf, ed., North-Holland, Amsterdam, 45, 326, 2003.
- [5] V.S. Letokhov, *Zh. Eksp. Teor. Fiz.*, 53, 1442, (1967); *Sov. Phys. J. Exp. Theor. Phys.*, 26, 835, (1968).
- [6] V.M. Markushev, V.F. Zolin, and Ch.M. Briskina, *Sov. J. Quantum Electron.*, 16, 2, 281, (1986).
- [7] V.M. Markushev, N.É. Ter-Gabriélyan, Ch.M. Briskina, V.R. Belan, and V.F. Zolin, *Sov. J. Quantum Electron.*, 20, 773, (1990).
- [8] Ch.M. Briskina, V.M. Markushev, and N.E. Ter-Gabrielyan, *Sov. J. Quantum Electron.*, 26, 10, 923, (1996).
- [9] L. Sirbu, V.V. Ursaki, I.M. Tiginyanu, K. Dolgaleva, and R.W. Boyd, *Phys. Stat. Sol. (RRL)*, 1, R13, (2007).
- [10] L. Sirbu, V.V. Ursaki, I.M. Tiginyanu, K. Dolgaleva, and R.W. Boyd, *J. Opt. A: Pure Appl. Opt.*, 9, 401, (2007).
- [11] D.S. Wiersma, M.P. van Albada, and A. Lagendijk, *Rev. Sci. Instrum.*, 66, 5473, (1995).
- [12] M.B. van der Mark, M.P. van Albada, and A. Lagendijk, *Phys. Rev. B*, 37, 3575, (1988).
- [13] B. Henderson and G.F. Imbusch, *Optical Spectroscopy of Inorganic Solids*, Oxford University Press, USA, 672, 2006.